Int. J. Heat Mass Transfer. Vol. 29, No. 7, pp. 1041–1049, 1986
Printed in Great Britain

0017–9310/86 $3.00 + 0.00
Pergamon Journals Ltd.

One-dimensional simulation of the thermal structure of urban atmospheres

A. YOSHIDA and T. KUNITOMO

Department of Engineering Science, Faculty of Engineering, Kyoto University, Yoshida Honmachi, Sakyo-ku Kyoto 606, Japan

(*Received* 10 *June* 1985 *and in final form* 27 *December* 1985)

Abstract—In order to elucidate the thermal structure of the atmosphere in urban areas, a one-dimensional numerical simulation is performed. Particular attention is paid to the effects of the earth surface condition, aerosols and artificial heat release. The results indicate that the temperature in urban areas is generally higher than in rural areas and that the inversion layer near the earth surface in urban areas disappears at night in the winter season due to surface roughness and artificial heat release. A considerable temperature difference is formed in rural and urban areas for several hours before and after sunset. Aerosols have a great effect in daytime and the maximum effect of the aerosol diameter is found for the case of the diameter nearly equalling the wavelength of visible light.

1. INTRODUCTION

THE METEOROLOGICAL conditions in urban areas are different from those in rural areas. In urban areas, a high temperature region is frequently formed and is called the heat island. This phenomenon is particularly noticeable in a big city and is caused by the artificial thermal environment. Conceivable causes are: a shortage of vegetation, asphalt pavements, concrete buildings and discharge of heat and aerosols from factories. A number of studies have been carried out on the thermal structure of urban atmospheres [1–6]; a problem which combines various factors in a complicated way. In the previous studies, however, several factors have not been included. In some cases, the adopted parameters are not in agreement with those in the real environmental system. Furthermore, the radiative heat transfer, which is regarded as important when the thermal structure of the urban atmosphere is discussed, has not been considered properly, since the effect could not be easily incorporated into the calculation. Therefore, it was difficult to gain a correct understanding. However, the study by Yoshida and Kunitomo [7] recently treated the radiative heat transfer exactly and clarified the effect of aerosols. However, heat transfer mechanisms other than radiation were not included in ref. [7]. Therefore, in this paper, we took up various factors which play important roles in urban meteorological phenomena and carried out a one-dimensional numerical simulation taking full consideration of radiative heat transfer and heat balance. With regard to aerosols, it is considered that they have a great influence on the thermal structure of the atmosphere when their concentration is increased.

With this in mind, we examined thoroughly the effects of size distribution, complex refractive index and relative humidity. Polluting gases such as SO_2 and NO_x may have influences upon the thermal structure when their concentrations are very high. But we do not need to consider such an unrealistic condition. In the following, we supposed the urban and rural atmospheric models to be connected with actual conditions and examined synthetically the effects of various parameters. A revised analytical method is proposed to treat the surface boundary layer and to determine the surface temperature.

2. THEORETICAL ANALYSIS

2.1. *Model*

The physical model of the atmosphere is shown in Fig. 1.

To analyze the problem, the following assumptions and conditions are introduced.

1. The atmosphere and the soil layer are plane parallel and infinite and can be treated one-dimensionally.
2. The region between the atmospheric boundary and the soil layer from 2000 m above the ground to 50 cm below the surface is considered in this simulation. In the free atmosphere above an altitude of 2000 m the atmospheric variables are independent

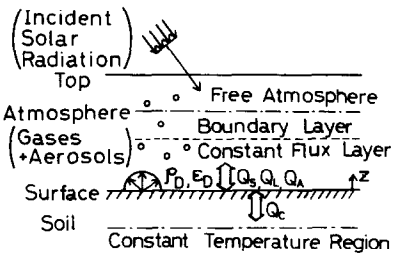

FIG. 1. Physical model for heat transfer in the atmosphere and the soil layer.

NOMENCLATURE

C aerosol concentration
C_s heat capacity of soil layer
c_p specific heat at constant pressure
d aerosol diameter
F integrated value of ϕ with z, equation (10)
f_c Coriolis factor
K turbulent eddy diffusivity
k_c Von Karman constant
L Monin–Obukov stability length
l evaporation heat
M moisture parameter at the earth surface, equation (15)
m_p aerosol source strength
$\hat{n}$ complex refractive indices of aerosol
Q_A, Q_C, Q_L, Q_S, Q_R artificial heat flux, conductive heat flux, latent heat flux, sensible heat flux and radiative heat flux at the earth surface, respectively
q specific humidity
q_a specific humidity at the top of the surface boundary layer
q_s saturated specific humidity at the earth surface
R atmospheric heating rate by radiative heat flux
Ri Richardson number
T temperature of the atmosphere
T_s temperature of soil layer
T_0 temperature at the earth surface
T_{200} temperature of the atmosphere at an altitude of 200 m
t time
u, v wind velocity (x, y component)
u_g, v_g geostrophic wind (x, y component)
u_* friction velocity
z vertical coordinate
z_0 surface roughness.

Greek symbols

ε_D emittance at the earth surface
θ potential temperature
θ_* frictional potential temperature
κ thermal diffusivity of soil layer
λ thermal conductivity of soil layer
ρ density of the atmosphere
ρ_D reflectance (albedo) of the earth surface
ϕ_m, ϕ_h vertical profile parameters for velocity and potential temperature, respectively, equation (11).

of time. The temperature in the soil layer below 50 cm is assumed to be constant during the simulation period of a few days. The surface boundary layer at an altitude of 50 m is supposed to be the layer of constant vertical momentum, heat and mass flux.

3. Local thermodynamic equilibrium is attained.
4. Clouds are not considered. Phase change and chemical reaction can be neglected.
5. Gases (H_2O, CO_2, O_3) and aerosols are included in the calculation of radiative heat transfer. In the daytime, the solar and atmospheric radiations are partially absorbed at the earth surface. This absorbed energy is transferred to the atmosphere by convection (sensible and latent heat) and radiation, and to the soil by conduction. In urban areas, the artificial heat release is also introduced.
6. The area of middle latitude is considered. The simulation is carried out for summer and winter seasons.

2.2. *Basic equations*

Under the above assumptions and conditions, the basic equations are introduced for the three different regions.

(i) Atmospheric boundary layer ($50 \leqslant z \leqslant 2000$ m)

$$\frac{\partial u}{\partial t} = f_c(v - v_g) + \frac{\partial}{\partial z}\left(K_m \frac{\partial u}{\partial z}\right) \tag{1}$$

$$\frac{\partial v}{\partial t} = f_c(u_g - u) + \frac{\partial}{\partial z}\left(K_m \frac{\partial v}{\partial z}\right) \tag{2}$$

$$\frac{\partial \theta}{\partial t} = \frac{\partial}{\partial z}\left(K_h \frac{\partial \theta}{\partial z}\right) + R \tag{3}$$

$$\frac{\partial q}{\partial t} = \frac{\partial}{\partial z}\left(K_q \frac{\partial q}{\partial z}\right) \tag{4}$$

$$\frac{\partial C}{\partial t} = \frac{\partial}{\partial z}\left(K_c \frac{\partial C}{\partial z}\right). \tag{5}$$

The calculation method of the atmospheric heating rate R by the radiative heat flux in equation (3) is given by Yoshida and Kunitomo [7]. The turbulent eddy diffusivities, Ks, are adopted from the paper by O'Brien [8] and it is assumed that $K_h = K_q = K_c$. For the condition of $K_m < 0.1$ m^2 s^{-1}, it is assumed that the wind velocity components, u and v, are equal to u_g and v_g, respectively.

(ii) Surface boundary layer ($0 \leqslant z \leqslant 50$ m)

$$U = u_* F_m / k_c \tag{6}$$

$$\theta = \theta_0 + \theta_* F_h / k_c \tag{7}$$

$$q = q_0 + q_* F_q / k_c \tag{8}$$

$$C = C_0 + C_* F_c / k_c \tag{9}$$

where $k_c = 0.4$ and $U = \sqrt{u^2 + v^2}$. In this layer the

wind direction does not change and the subscript 0 means values at the earth surface. u_*, θ_*, q_* and C_* do not change with the altitude in this surface boundary layer. The momentum flux and the heat flux are u_*^2 and $u_*\theta_*$, respectively. The assumption of $F_h = F_q = F_c$ is adopted. F_m and F_h are expressed by

$$F_m = \int_{z_0}^{z} \frac{\phi_m}{z}\,dz, \quad F_h = \int_{z_0}^{z} \frac{\phi_h}{z}\,dz \tag{10}$$

where

$$\phi_m = \frac{k_c z}{u_*}\frac{\partial U}{\partial z}, \quad \phi_h = \frac{k_c z}{\theta_*}\frac{\partial \theta}{\partial z}$$

ϕ_m and ϕ_h are formulated by Kondo [9] and are the functions of the Monin–Obukov stability length. The turbulent eddy diffusivities in this layer are defined by the following expressions

$$K_m = k_c u_* z/\phi_m, \quad K_h = k_c u_* z/\phi_h. \tag{12}$$

(iii) Soil layer ($-50 \leqslant z \leqslant 0$ cm)

$$\frac{\partial T_s}{\partial t} = \kappa \frac{\partial^2 T_s}{\partial z^2}. \tag{13}$$

The boundary conditions are as follows.

(a) At the top of the atmospheric boundary layer ($z = 2000$ m):

$$u, v, \theta, q, C = \text{const.} \tag{14}$$

where $u = u_g$ and $v = v_g$.

(b) At the top of the surface boundary layer ($z = 50$ m): u, v, θ, q and C are continuous.

(c) At the earth surface ($z = 0$):

$$q - q_a = M(q_s - q_a) \tag{15}$$

$$K_c(\partial C/\partial z) = -m_p \tag{16}$$

$$U = 0 \tag{17}$$

$$\rho c_p K_h \frac{\partial \theta}{\partial z} + l\rho K_q \frac{\partial q}{\partial z} - \lambda \frac{\partial T_s}{\partial z} + Q_R + Q_A = 0. \tag{18}$$

(d) At $z = -50$ cm in the soil layer

$$T_s = \text{const.} \tag{19}$$

It is assumed that the earth surface can not store the energy and that the surface temperature is obtained by the energy balance equation (18). In equation (18) the radiative heat flux Q_R is given from the paper by Yoshida and Kunitomo [7]. It is difficult to determine the reliable value of the moisture parameter M in equation (15) as suggested by Halstead *et al.* [10], but it is possible to discuss quantitatively the effect of latent heat flux at the surface. For example: when $M = 0$, latent heat flux is zero; when $M = 1$, the surface moisture is saturated and latent heat flux probably has the maximum value. So the procedure adopted in this paper to consider the effect of the moisture transfer is appropriate for the simulation.

The effects of the phase change between water and water vapor are discussed briefly. Once condensation begins, buoyancy occurs because the air particle is warmed up by the heat of condensation. Because of this, the condensation phenomenon is further intensified. However, when the condensation proceeds to some extent and the condensation layer becomes thick, the cooling action due to infra-red radiation takes effect. The surface temperature is also changed under the influence of the infra-red radiation flux. The interaction between the condensation layer and the ground surface must be considered too. The region that the effect of the condensation phenomenon extends to is closely connected with the atmospheric stability. The possibility of condensation in urban areas is usually smaller than that in rural ones, because in the city the atmosphere is often in an unstable condition and the relative humidity is lower. In the following calculated results are few cases where condensation occurs. The mechanism of condensation from its appearance to its disappearance will be included in a future simulation model.

2.3. *Calculation procedure*

The partial differential equations (1)–(5) and (13) were solved numerically by a finite-difference technique. The implicit Crank–Nicolson method could be used with good stability. A time step of 30 min was adopted. After 39 h of the preceding calculation from 0900 h, the final calculation was started at 0000 h on the third day and was continued for 24 h. As the results of this final calculation were not affected by the initial conditions, they were used for discussion. The grid spaces in the atmosphere were 100 m above an altitude of 1000 m, and 50 m below an altitude of 1000 m; those in the soil layer were 2.5–5 cm.

In order to obtain the surface temperature, equation (18) must be solved. However, (18) is a function of the Monin–Obukov length L where the surface temperature is included implicitly. The following equation is given from the definition of the bulk Richardson's number

$$Ri = \frac{z}{L} \cdot F_h \cdot F_m^{-2}. \tag{20}$$

Then the surface temperature was determined by solving equation (18) and (20) simultaneously.

3. RESULTS AND DISCUSSION

3.1. *Effects of parameters*

The thermal structural feature of urban atmospheres is affected by various complicated factors. In order to know the effect of each parameter, the value of the specified parameter was changed while the other parameters were fixed. The results at 1300 h when the highest temperature usually appears and the results at 0500 h in summer and at 0700 h in winter when the lowest temperature appears were chosen for discussion. The

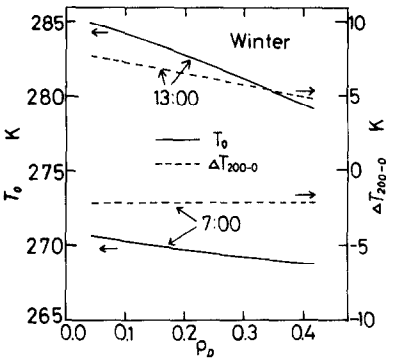

FIG. 2. Effect of the reflectance (albedo) at the ground surface for the solar radiation on the surface temperature and the air temperature.

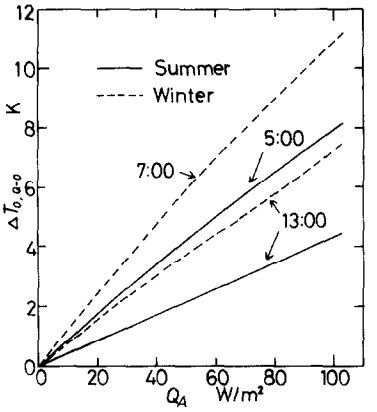

FIG. 4. Effect of the artificial heat release on the surface temperature.

boundary conditions for temperatures were

θ = 309.0 K (summer), 286.1 K (winter) at z = 2000 m

T_s = 297.0 K (summer), 277.0 K (winter) at z = −50 cm.

Figure 2 shows the effect of albedo ρ_D for solar radiation in winter. The earth surface was treated as the gray body; ΔT_{200-0} is the difference between T_0 and T_{200}. In the daytime the surface temperature decreases with the increase of ρ_D, due to the decrease of the absorbed solar energy at the surface. Due to the decrease of the temperature difference with the increase of ρ_D, sensible heat flux at the surface decreases too. This difference was not found between the summer and the winter seasons. The value of ρ_D in urban areas is usually smaller than that in rural areas, due to the multiple absorption among buildings. This may contribute a little to the higher temperature near the surface in urban areas.

Figure 3 shows the effect of surface emittance ε_D in the infra-red region in winter. The surface temperature rises with the decrease of the emittance. The upper air temperature is not affected. In the infra-red region almost all surfaces are regarded as black ($\varepsilon_D \simeq 1.0$) and the effect is supposed to be small.

Figure 4 shows the effect of the artificial heat release. $\Delta T_{0,Q-0}$ is the difference of the surface temperature between two cases: artificial heat released and artificial heat not released. The variation of the heat release with time was not considered. The heat release was assumed to occur at the earth surface. The surface temperature rises almost linearly with the increase of the artificial heat release. The surface temperature is more sensitive to the artificial heat release at night or in winter, in comparison with the daytime or summer, respectively. This result is caused by the situation that the ratio of the artificial heat to the other energy sources at the surface becomes larger at night or in winter. Actually the artificial heat release is 10–100 W m^{-2} in a big city and its effect is supposed to be very large. Figure 5 shows the change of the vertical distribution of the air temperature with the artificial heat release. The result at dawn in winter is shown since it is greatly affected by the artificial heat. With the increase of the artificial heat, the strength of the inversion layer near the earth surface (e.g. the difference between the surface and the peak temperature) becomes weaker and the peak altitude of the inversion falls. Then the atmosphere becomes unstable and the convective heat exchange becomes

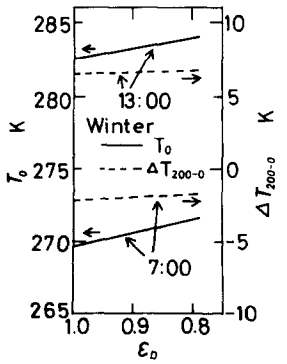

FIG. 3. Effect of the emittance at the ground surface for the infra-red radiation on the surface temperature and the air temperature.

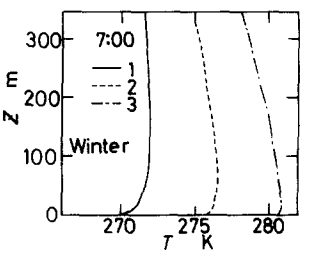

FIG. 5. Effect of the artificial heat release on the vertical distribution of the air temperature. The notations of 1, 2 and 3 mean Q_A = 0, 50 and 100 W m^{-2}, respectively.

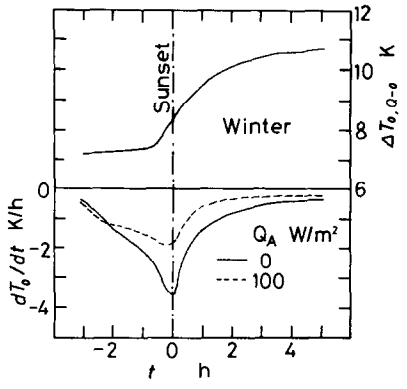

FIG. 6. Effect of the artificial heat release on the change of the surface temperature with time before and after sunset.

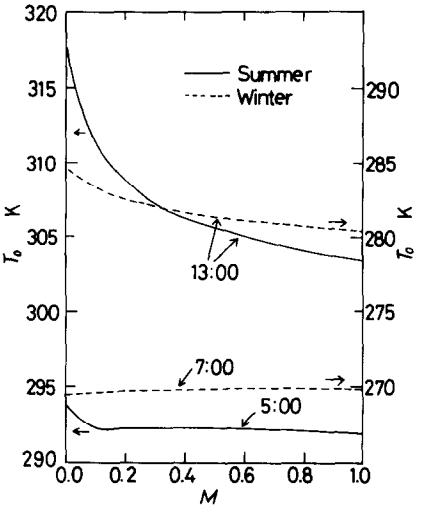

FIG. 8. Effect of the evaporation from the ground surface on the surface temperature.

active. The artificial heat has, therefore, a large influence not only on the surface temperature but also on the upper air temperature. In the lower part of Fig. 6, the variation of the surface temperature with time, dT_0/dt, is shown. The difference of dT_0/dt between two cases of $Q_A = 0$ and $Q_A = 100$ W m^{-2} becomes large in several hours before and after sunset and the maximum increase rate of the temperature difference is also obtained at that time. This result agrees with the observation that the phenomenon of the heat island grows rapidly just before and after sunset [11].

Figure 7 shows the effect of the surface roughness in winter. With the increase of the surface roughness z_0, the surface temperature falls in the daytime and rises slightly at night. With the increase of z_0, the turbulent intensity in the atmosphere becomes strong and the mixing with the upper air becomes active. The difference between the surface temperature and the upper air temperature becomes small, which results in the disappearance of the inversion layer. The surface roughness has a larger influence on the surface temperature in the daytime or in summer than at night or in winter, respectively, since in the former case the heat transfer by convection is active.

Figure 8 shows the effect of evaporation at the surface, i.e. the moisture parameter M. When $M = 0$, the surface is dry and when $M = 1$ it is wet. The amount of the heat transfer by latent heat has a peak at $M = 1$. Since the surface in urban areas is covered with concrete and asphalt instead of vegetation, the value of M is usually smaller than that in rural areas. With the increase of M, latent heat flux increases and the surface temperature decreases due to the energy balance. Since the heat is transferred by latent heat from the surface in the cases of summer and daytime more actively than in the cases of winter and night-time, respectively, the effect of the wetness at the surface is stronger in the former cases—especially in the case of small values of M, e.g. in the case of urban areas, the effect is also strong.

Figure 9 shows the effects of the thermal diffusivity κ

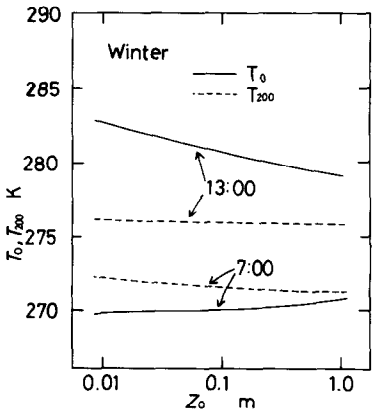

FIG. 7. Effect of the surface roughness on the air temperature and the surface temperature.

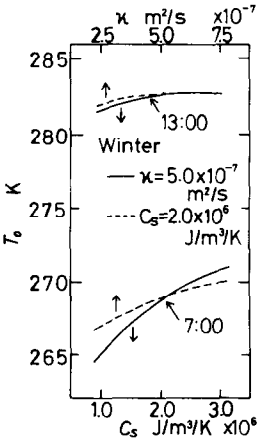

FIG. 9. Effect of the thermal properties of the soil layer (i.e. thermal diffusivity and heat capacity) on the surface temperature.

and the heat capacity C_s of the soil layer in winter. At night, with the increase of κ and C_s, the surface temperature increases since the conduction in the soil is the dominating factor. When the thermal diffusivity is large, the amplitude of the fluctuation of the surface temperature becomes small. When the heat capacity is large, it becomes small too. The thermal properties depend on the percentage of moisture content and the porosity. The values of $\kappa = 5.0 \times 10^{-7}$ m^2 s^{-1} and $C_s = 2.0 \times 10^6$ J m^{-3} K^{-1} correspond to the wet soil.

Figure 10 shows the effect of the geostrophic wind in winter. The y-component, v_g, is assumed to be zero. With the increase of the geostrophic wind velocity, the surface temperature in the daytime decreases and that at night increases. Furthermore, the difference between the upper air temperature and the surface temperature becomes small. This is caused by the fact that the convective heat transfer becomes activated by the stronger geostrophic wind, i.e. the stronger wind nearer the surface.

In the following the results of the effect of aerosols are shown. The values of 0.4 μm and 0.375 μg m^{-2} s^{-1} and Model 2 [7] were adopted for the aerosol diameter and the source strength and for the model of the refractive indices of aerosols, unless otherwise stated.

Figure 11 shows the effect of the diameter and size distribution of aerosols. $\Delta T_{0,p}$ and $\Delta T_{200,p}$ indicate the difference in the surface temperature and that in the temperature at an altitude of 200 m, respectively, caused by the existence of aerosols. The volume concentration was kept constant in the calculation. Since aerosols are not generally monodispersive, the effect of the size distribution was considered and is shown by the results at 1300 h in winter with the marks of Junge 1, Junge 2 and Haze L. The size distributions are as follows; Junge 1: $n(d) = c_1 d^{-4}$ ($0.2 \leqslant d \leqslant 2.0$ μm); Junge 2: $n(d) = c_1 d^{-4}$ ($0.1 \leqslant d \leqslant 4.0$ μm); Haze L: $n(d) = c_2 d^2 \times \exp[-17.059 d^{1/2}]$, where c_1 and c_2 are constants. The representative diameters for scattering, $d_{32} (\equiv \int d'^3 n(d') \mathrm{d}d' / \int d'^2 n(d') \mathrm{d}d')$, are 0.38 μm in Junge 1 and Haze L and 0.40 μm in Junge 2. In the daytime the surface temperature falls since the solar beam energy is lost by the scattering and absorption

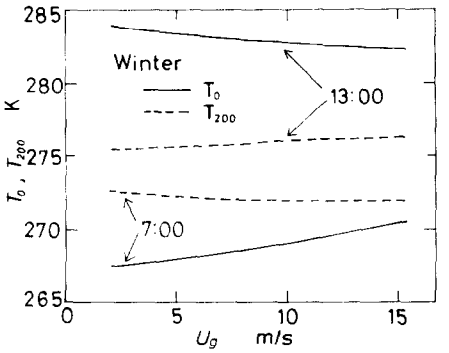

FIG. 10. Effect of the geostrophic wind on the surface temperature.

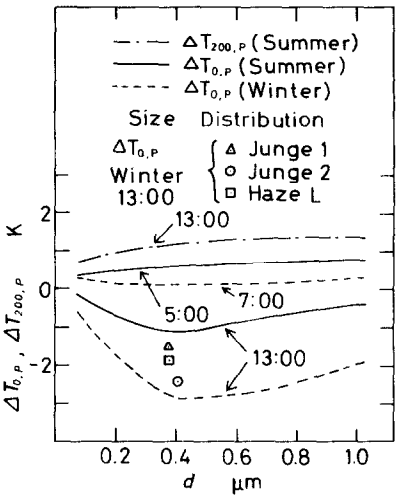

FIG. 11. Effect of the diameter and the size distribution of aerosols on the surface temperature and the air temperature.

of aerosols although the diffuse light increases. The maximum effect is found at the aerosol diameter around 0.4 μm. This is caused by the fact that the effect of the scattering by aerosols becomes large; furthermore the forward scattering becomes dominant with the increase of diameter [7]. The effect of diameter is weakened by the size distribution. The effect of aerosols in the daytime is stronger in winter than in summer because the solar zenith angle is smaller and the optical depth is larger. The temperature of the higher altitude tends to rise more, because of the absorption of solar energy by aerosols. Early in the morning, the effect of aerosols is weak but the surface temperature rises because the downward infra-red energy from the atmosphere to the surface increases at the rate of 2–4%. Since the temperature and the infra-red atmospheric radiation are higher at night in summer than in winter, the effect of aerosols is stronger in the former case.

Figure 12 shows the effect of the difference in the

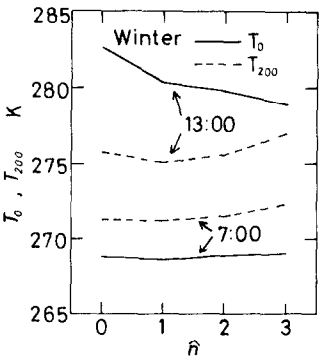

FIG. 12. Effect of the difference in the models of the complex refractive indices of aerosols on the surface temperature and the air temperature. The number on the axis of abscissa, 0, 1, 2 and 3 mean no existence of aerosols, Model 1, Model 2 and Model 3 [7].

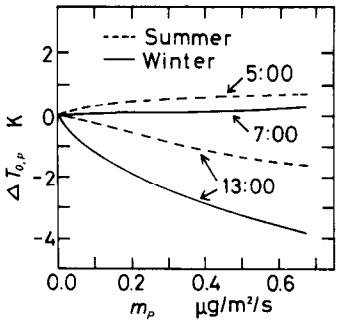

FIG. 13. Effect of the aerosol source strength.

models of the complex refractive indices. Models 1, 2 and 3 [7] are assumed to correspond to the clean atmosphere, the urban atmosphere and the especially polluted atmosphere, respectively. At night the effect of the models is weak. However, in the daytime, the large difference is caused because the imaginary parts of the complex refractive indices in the visible region are extremely different among the models.

Figure 13 shows the effect of the aerosol source strength m_p, where the effect becomes large with the increase of m_p. Figure 14 shows the beam solar radiation F_b and the diffuse solar radiation F_d at the surface. It is understood that the depression of the surface temperature is mainly caused by the decrease of F_b. F_d is kept nearly constant when $m_p > 0.2$ μg m^{-2} s^{-1}.

Table 1 shows the effect of the relative humidity which causes the variations of the diameter and the complex refractive indices of aerosols. $\Delta T_{0,f}$ is the difference between the surface temperatures that are obtained by either considering or ignoring the humidity effect; $\Delta T_{200,f}$ is the same difference at an altitude of 200 m. The moisture parameters M adopted in summer and in winter were 0.3 and 0.2,

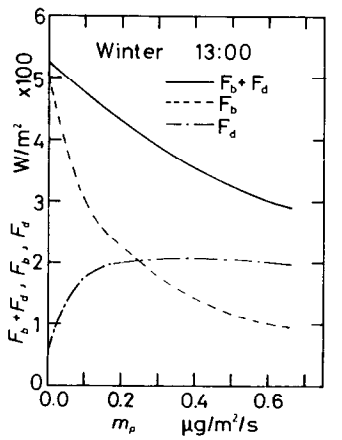

FIG. 14. Relation between the aerosol source strength and the components of the downward solar radiation at the surface. F_b and F_d mean the solar beam radiation and the diffuse radiation.

Table 1. Effect of the relative humidity in the atmosphere

		Summer	Winter
0500	$\Delta T_{0,f}$	+1.2	+0.4
	$\Delta T_{200,f}$	+0.2	+0.1
1300	$\Delta T_{0,f}$	−1.9	−1.1
	$\Delta T_{200,f}$	−0.8	−0.4

respectively. At night the surface was almost saturated. In the daytime the relative humidities at the surface were about 70% in summer and 60% in winter, respectively. Since in the summar the relative humidity is high, the effect is strong. In the daytime, the temperatures fall since the effect of the increase of aerosol diameter, i.e. the increase of scattering, exceeds that of the decrease of the imaginary part of the complex refractive indices [7]. At night the temperature rises due to the increase of aerosol diameter, i.e. the increase of emission. However, since the relative humidity is generally low in urban areas, this effect is not so strong.

3.2. *Combined effect of various parameters*

In the following, the combined effect of various parameters is examined by adopting typical combinations for urban and rural areas. The values of parameters for both areas are shown in Table 2; the boundary conditions in urban and rural areas were the same. The results are shown in Figs. 15–17. Figure 15 shows the variations of the surface temperatures in 24 h in both areas. The large difference at night between the two areas arises in the few hours before and after sunset, and is kept nearly constant until sunrise; this agrees well with observation [11]. The peak temperature of urban areas in the daytime occurs a little later than that in rural areas. In Figs. 16 and 17 the temperature distributions in winter and summer are shown, respectively, where the numbers in

Table 2. Parameters in rural and urban areas

Parameter	Rural	Urban
ρ_D	0.20	0.15
ε_D	1.00	1.00
M	0.3(s) 0.2(w)	0.1
z_0(m)	0.01	1.0
Q_A (W m^{-2})	0.0	35.0(s) 50.0(w)
U_g(m s^{-1})	9.0(s) 12.0(w)	9.0(s) 12.0(w)
κ (m^2 s^{-1})	5.0×10^{-7}	7.5×10^{-7}
C_s (J m^{-3} K^{-1})	2.0×10^{6}	2.0×10^{6}
d	—	Haze L
$\hat{n}$	—	Model 2
m_p(μg m^{-2} s^{-1})	0.0	0.375

s and w indicate summer and winter seasons, respectively.

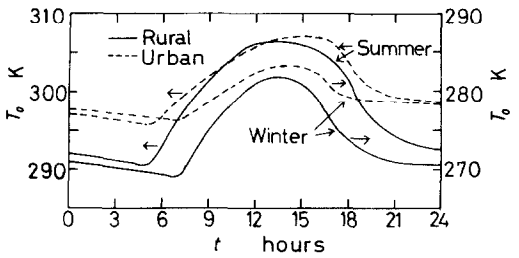

FIG. 15. Variation of the surface temperature over 24 h.

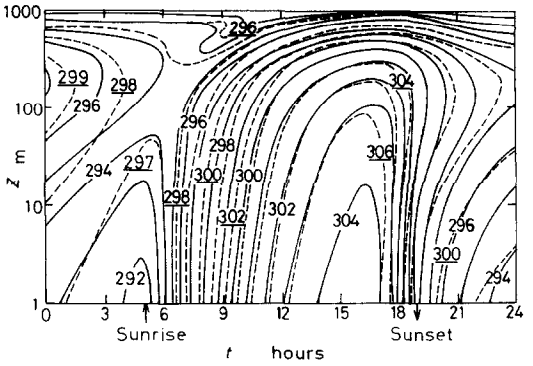

FIG. 17. Air temperature distribution in summer. —— rural model; – – – urban model.

the figure indicate the temperatures and the numbers underlined correspond to the case of urban areas. The temperatures in urban areas are usually higher than those in rural areas. A large difference between the two areas is found at night. In both figures, the weak inversion layers are found from sunrise to noon, and these are caused by the development of the boundary layer. In winter, the inversion layer at night near the earth surface almost disappears in urban areas; this is mainly due to the effects of large artificial heat release and large surface roughness. In the daytime, the temperature difference between the two areas is small because the surface roughness and the aerosol act as a brake on the temperature increase in urban areas.

4. CONCLUSIONS

The thermal structure of urban atmospheres is examined by one-dimensional simulation. The results obtained are summarized as follows:

1. At night all parameters considered in the simulation cause the increase of the surface temperature in urban areas. The effects of the artificial heat release and the thermal properties of the soil layer are relatively stronger than those of the other parameters. The inversion layer near the surface at night is disturbed mainly by the surface roughness and the artificial heat release.

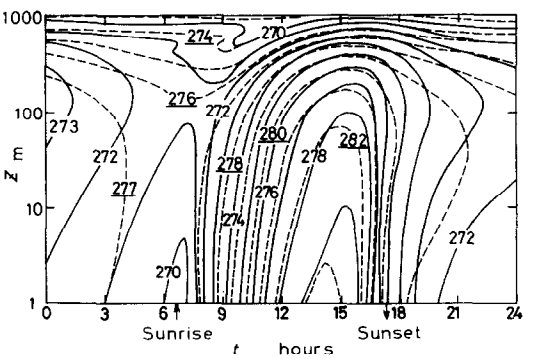

FIG. 16. Air temperature distribution in winter. —— rural model; – – – urban model.

2. In the daytime, the large surface roughness and the aerosol decrease the surface temperature in urban areas. On the other hand, the large artificial heat release, the small evaporation rate at the surface and the small reflectance of the surface cause the increase of the surface temperature.
3. The effect of aerosols is strong in the daytime. The maximum effect of the aerosol diameter is found at a diameter of around 0.4 μm. The complex refractive indices affect significantly the temperature in the daytime. At night the aerosol effect is weak. When the relative humidity in the atmosphere is high, the dependency of the diameter and the complex refractive indices on the relative humidity must be taken into consideration, otherwise it leads to the wrong results.
4. The temperature in urban areas is usually higher than that in rural areas. A larger difference between urban and rural areas is found in winter and at night than in summer and in the daytime, respectively. The large difference at night between two areas arises in the few hours before and after sunset.

REFERENCES

1. R. W. Bergstrom and R. Viskanta, Modeling of the effects of gaseous and particulate pollutants in the urban atmosphere (Part I). Thermal structure, *J. appl. Met.* **12,** 901–912 (1973).
2. M. A. Atwater, Thermal effects of urbanization and industrialization in the boundary layer: a numerical study, *Boundary-Layer Met.* **3,** 229–245 (1972).
3. L. O. Myrup, A numerical model of the urban heat island, *J. appl. Met.* **8,** 908–918 (1969).
4. K. E. Torrance and J. S. W. Shum, Time-varying energy consumption as a factor in urban climate, *Atmos. Environ.* **10,** 329–337 (1976).
5. T. Sasamori, A numerical study of atmospheric and soil boundary layers, *J. atmos. Sci.* **27,** 1122–1137 (1970).
6. W. G. Zdunkowski, R. M. Welch and J. Paegle, One-dimensional numerical simulation of the effects of air pollution on the planetary boundary layer, *J. atmos. Sci.* **33,** 2399–2414 (1976).
7. A. Yoshida and T. Kunitomo, Theoretical investigation of the effects of aerosol characteristics on the radiative

heat transfer in the atmospheric boundary layer, *Bull. J.S.M.E.* **26**, 1929–1935 (1983).
8. J. O'Brien, On the vertical structure of the eddy exchange coefficient in the planetary boundary layer, *J. atmos. Sci.* **27**, 1213–1215 (1970).
9. J. Kondo, Air-sea bulk transfer coefficients in diabatic condition, *Boundary-Layer Met.* **9**, 91–112 (1975).
10. M. H. Halstead, R. L. Richman, W. Covey and J. D. Merryman, A preliminary report on the design of a computer for micrometeorology, *J. Met.* **14**, 308–325 (1957).
11. T. R. Oke and G. B. Maxwell, Urban heat island dynamics in Montréal and Vancouver, *Atmos. Environ.* **9**, 191–200 (1975).

SIMULATION MONODIMENSIONNELLE DE LA STRUCTURE THERMIQUE DE L'ATMOSPHERE URBAINE

Résumé—On construit une simulation numérique monodimensionnelle de l'atmosphère urbaine pour clarifier la structure thermique. Une attention particulière est portée aux effets de la condition à la surface du sol, des aérosols et des sources de chaleur artificielles. Les résultats montrent que le température dans un site urbain est généralement plus élevée que dans un site rural et que la couche d'inversion près du sol en zone urbaine disparait pendant la nuit d'hiver à cause de la rugosité de surface et de la création de chaleur artificielle. Une différence considérable de température apparait entre sites rural et urbain pour quelques heures avant et après le lever du soleil. L'aérosol a un effect dans la journée et un maximum d'effet du diamètre est trouvé lorsque le diamètre est proche de la longueur d'onde de la lumière visible.

EINDIMENSIONALE SIMULATION DER THERMISCHEN STRUKTUR DER ATMOSPHÄRE ÜBER STÄDTISCHEN GEBIETEN

Zusammenfassung—Zur Beschreibung der thermischen Struktur der Atmosphäre über städtischen Gebieten wurde eine eindimensionale numerische Simulation durchgeführt. Besonders berücksichtigt wurden die Einflüsse von Eigenschaften der Erdoberfläche, von Aerosol und von künstlicher Wärmefreisetzung. Die Ergebnisse zeigen, daß die Temperatur über städtischen Gebieten im allgemeinen höher ist als über ländlichen Gebieten und sich die Inversionsschicht in der Nähe der Erdoberfläche über städtischen Gebieten in Winternächten—bedingt durch die Oberflächenrauhheit und künstliche Wärmefreisetzung—auflöst. Erhebliche Unterschiede zeigen die Temperaturen in ländlichen und städtischen Gebieten für einige Stunden vor und nach Sonnenuntergang. Das Aerosol hat tagsüber einen großen Einfluß, wobei die Partikelgröße dann eine besonders große Rolle spielt, wenn ihr Durchmesser nahezu gleich groß wie die Wellenlänge des sichtbaren Lichtes ist.

ОДНОМЕРНАЯ МОДЕЛЬ ТЕПЛОВОЙ СТРУКТУРЫ АТМОСФЕРЫ ГОРОДА

Аннотация—Для определения тепловой структуры атмосферы в городской зоне проведено одномерное моделирование. Особое внимание уделено учету условий на поверхности земли, аэрозолей и источников тепла, созданных человеческой деятельностью. Результаты показывают, что в городской зоне температура обычно выше, чем в сельской, и инверсионный слой вблизи земной поверхности исчезает зимой в ночное время из-за неровностей рельефа и вышеупомянутых источников. В течение нескольких часов до и после захода солнца в городской и сельской зонах существует заметное различие температур. Влияние аэрозолей велико в дневное время и максимально, когда диаметр частиц близок к длине волны видимого излучения.